PLOS ONE

RESEARCH ARTICLE

Identification of druggable targets from the interactome of the Androgen Receptor and Serum Response Factor pathways in prostate cancer

Haleema Azam[1,2], Colin Veale[1,2], Kim Zitzmann[1,2], Simone Marcone[3], William M. Gallagher[1,2], Maria Prencipe[1,2]*

1 Cancer Biology and Therapeutics Laboratory, Conway Institute of Biomolecular and Biomedical Research, University College Dublin, Dublin, Ireland, **2** School of Biomolecular and Biomedical Science, University College Dublin, Dublin, Ireland, **3** Department of Surgery, Trinity Translational Medicine Institute, Trinity St. James's Cancer Institute, Trinity College Dublin, Dublin, Ireland

* maria.prencipe@ucd.ie

Citation: Azam H, Veale C, Zitzmann K, Marcone S, Gallagher WM, Prencipe M (2024) Identification of druggable targets from the interactome of the Androgen Receptor and Serum Response Factor pathways in prostate cancer. PLoS ONE 19(12): e0309491. https://doi.org/10.1371/journal.pone.0309491

Editor: Keisuke Hitachi, Fujita Health University, JAPAN

Received: August 13, 2024

Accepted: November 23, 2024

Published: December 13, 2024

Data Availability Statement: The mass spectrometry proteomics data for this study are publicly available from the Dryad repository (https://doi.org/10.5061/dryad.63xsj3vbb).

Funding: MP, HA & CV: Science Foundation Ireland (https://www.sfi.ie/) (18/SIRG/5510); KZ: Irish Research Council (https://research.ie/) (GOIPG/2023/4311). The founders did not play any role in the study design, data collection and

Abstract

Background

The Androgen Receptor (AR) pathway is crucial in driving the progression of prostate cancer (PCa) to an advanced state. Despite the introduction of second-generation AR antagonists, such as enzalutamide, majority of patients develop resistance. Several mechanisms of resistance have been identified, including the constitutive activation of the AR pathway, the emergence of AR spliced variants, and the influence of other signalling pathways. The Serum Response Factor (SRF) was previously identified as a possible player of resistance involved in a crosstalk with the AR signalling pathway. Elevated SRF levels in PCa patients were associated with disease progression and resistance to enzalutamide. However, the molecular mediators of the crosstalk between SRF and AR still need to be elucidated. The objective of this study was to identify common interactors of the AR/SRF crosstalk as therapeutic targets.

Methods

Here we used affinity purification mass spectrometry (MS) following immunoprecipitation of SRF and AR, to identify proteins that interact with both SRF and AR. The list of common interactors was expanded using STRING. Four common interactors were functionally validated using MTT assays.

Results

Seven common interactors were identified, including HSP70, HSP0AA1, HSP90AB1, HSAP5, PRDX1 and GAPDH. Pathway analysis revealed that the PI3k/AKT pathway was the most enriched in the AR/SRF network. Moreover, pharmacological inhibition of several

analysis, decision to publish, or preparation of the manuscript.

Competing interests: The authors have declared that no competing interests exist.

proteins in this network, including HSP70, HSP90, PI3k and AKT, significantly decreased cellular viability of PCa cells.

Conclusions

This study identified a list of AR/SRF common interactors that represent a pipeline of druggable targets for the treatment of PCa.

Introduction

Castrate resistant prostate cancer (CRPC) grows independently of androgens. However, AR still plays a central role in driving progression to CRPC. Despite the addition of enzalutamide and other second-generation inhibitors of androgen biosynthesis, such as abiraterone acetate, for the treatment of advanced PCa, majority of patients develop resistance [1]. As new avenues of resistance to AR antagonists emerge, understanding AR's relationship with co-regulators will aid in finding targets to disrupt the AR pathway in CRPC. The study of the crosstalk between AR and other signalling pathways involved in the plasticity of AR transcriptional network will shed light on the molecular mechanism behind the transition from androgen-sensitive to CRPC. One way in which AR co-factors control its transcriptional activity is through regulating AR nuclear translocation [2]. SRF is a transcription factor that plays a key role in cytoskeleton organisation and is implicated in proteins' sub-cellular trafficking. Several studies have shown a crosstalk between SRF and AR [3–5]. In an isogenic model of CRPC, downregulation of SRF in the presence of DHT, stimulated an increase in AR transcriptional activity in the LNCaP Abl (androgen-independent), but not in the LNCaP parental cells (androgen-dependent), suggesting a negative feedback loop in the androgen-independent subline [4]. This negative feedback loop was also observed in patients' tissues from CRPC bone metastases, where a negative correlation occurred between AR and SRF protein expression [4]. Another study supporting the AR/SRF relationship showed that AR and SRF shared a gene signature of 158 genes that were androgen responsive in LNCaP and VCaP cell lines [6]. This gene signature was associated with poor outcome in patients [6]. Other studies on the relationship between AR and SRF, showed that inhibition of protein kinase N1 (PKN1), an SRF co-factor responsible for androgen mediated SRF transcriptional activity, led to decreased expression of SRF transcriptional targets and increased expression of AR transcriptional targets [5]. Additionally, Four and Half Lim domain 2 (FHL2), a protein that regulates AR activity [7, 8], is under the transcriptional control of SRF [9]. In line with these data, we have demonstrated that elevated SRF expression is associated with enzalutamide resistance in patients [10] and that inhibition of SRF reduces AR translocation to the nucleus [10]. Furthermore, a recent study demonstrates that androgens activate AR via the YAP/TAZ pathway, which is regulated by RhoA/SRF pathways in PCa cell lines. The same study showed that targeting SRF enhanced sensitivity to AR inhibition, which suggests a potential role for SRF and YAP/TAZ axis in regulating AR subcellular localisation [11]. Despite all the evidence supporting the crosstalk between SRF and AR, little is known about how SRF influences AR signalling and *vice versa*. Here we used co-immunoprecipitation (co-IP) and MS to identify common interactors of SRF and AR.

Materials and methods

Cell culture and reagents

LNCaP Parental cell line was routinely cultured in Advanced RPMI-1640 supplemented with 10% Fetal Bovine Serum (FBS), 100μl/mL streptomycin/100 U/mL penicillin and 1% Hepes. The isogenic LNCaP Abl subline was generated as previously described [12] and routinely cultured like the parental LNCaP but replacing FBS with Charcoal Stripped Serum. Cell lines were maintained at 37˚C in a humidified atmosphere and were routinely tested for mycoplasma. (5a,17b)-17-Hydroxy-androstan-3-one (DHT) was purchased from Sigma. JG-98, Ver-155008, Ganetespib, Ipatasertib and Alpesilib were purchased from MedChem Express.

Small-interfering RNA (siRNA) and plasmids' transfections

Two hundred thousand LNCaP Abl cells per well were seeded in 6 well plates and 1,500,000 cells in $10cm^3$ petri dishes. The following day, cells were transfected with siGENOME SMART pool targeting SRF, AR or siControl siRNA (all from Dharmacon), at a final concentration of 5nM, or with p-CGN SRF plasmid (Addgene plasmid 11977) or with p-HM6 empty vector at a final concentration of 1μg/μL, using lipofectamine 2000 (Invitrogen).

Co-Immunoprecipitation assay

Prior to cellular lysis, the antibody solution was prepared adding 2μg of either SRF (Novus, Biotechne), AR (Santa Cruz, California, US), Ms IgG or Rb IgG to 20μL A/G protein beads (Pierce) and 300μL PBS (Gibco). The beads/antibody mixture was incubated for an hour on a rotator at 4˚C. Following incubation, the mixture was washed with ice-cold lysis buffer 3 times. Cells were scraped with 500μL of lysis buffer (500μL of 1% Triton x100, 1mL of 20mM Tris-HCl pH7.5, 1.5mL of 150mM NaCl and 50μL of 1mM $MgCl_2$) and incubated for 10 mins on ice. 1mg of protein was added to the beads/antibody mix and incubated for 1 hour on a rotator at 4˚C. Samples were washed 3 times in ice-cold lysis buffer.

Peptide elution and digestion

Following Co-IP, the peptides in each sample were eluted with 60μL of ice-cold Elution Buffer I (0.012g Urea, 50μL of 1M Tris-HCl pH7.5) and 5μg/mL Trypsin (Promega, Seq Grade Modified) for 30 mins at RT. Samples were then centrifuged at 3000rpm for 30s. The supernatant was collected into a new Eppendorf tube, and 20μL of Elution Buffer II was added to each sample. This step was repeated twice. The supernatant was collected into a new centrifuge tube with a total volume of 110μL. Samples were left to digest overnight at 37˚C at 300rpm.

Liquid mass spectrometry (Bruker timsTOF Pro) and data analysis with MaxQuant

A Bruker timsTOF Pro MS (Bruker Daltonics, Bremen, Germany) connected to an EvoSep One chromatography system was used. The timsTOF Pro MS was run using positive ion polarity with TIMS (Trapped Ion Mobility Spectrometry) and PASEF (Parallel Accumulation Serial Fragmentation) modes. Accumulating ramp times for the TIMS were set at 100ms, with the ion mobility ranging from 0.6 to 1.6 Vs/cm. A mass range from 100 to 1,700 m/z was the set range to record the spectra of ions. The precursor MS Intensity Threshold was set to 2,500 and the precursor Target Intensity was set to 20,000. Each PASEF cycle included one MS ramp for precursor detection, accompanied by 5 PASEF MS/MS ramps and a total cycle time of 1.03s. Peptides were separated using reverse-phase C_{18} Endurance column (15cm x 150μm ID, C18,

1.9μm) using the Evosep pre-set 30 SPD method. Mobile phase A consisted of 0.1% (v/v) formic acid in water and phase B included 0.1% (v/v) formic acid in acetonitrile. Peptides were separated by increasing gradient of solvent B for 44 minutes with a flow rate of 0.5μL/min. MaxQuant v1.6.17.0 was used by applying the *Homo sapiens* subset of the Uniprot Swissprot database against the raw data. A contaminants database was included in the search and the 'Match Between Runs' and 'Label free quantification' were selected [13]. The minimum peptide length allowed was 7 amino acids. False discovery rate (FDR) for peptides was set at 0.01. Protein intensity of each identified protein was normalised to obtain the label free quantification intensity (LFQi) value. A ProteinGroups.txt output file generated by MaxQuant was used for subsequent data analysis. The mass spectrometry proteomics data have been deposited to the Dryad public repository (dataset identifier doi:10.5061/dryad.63xsj3vbb).

Perseus analysis

The ProteinGroups.txt file generated by MaxQuant was processed on Perseus (v1.6.12.0) [14]. Data was filtered based on the LFQi values, and possible contaminants and reverse protein hits were removed from the list of identified proteins. Proteins that were not present in at least two samples were excluded from the analysis. The data was then imported onto Excel, where the LFQi ratio between the AR endogenous/siRNA or SRFvector/siRNA were calculated. Proteins with an average LFQi ratio of 1.5 across 3 biological replicates for AR and 2 biological replicates for SRF were chosen. The same method was applied to AR endogenous + DHT/siRNA and SRF vector + DHT/siRNA.

STRING database search

A STRING (v11.5) database (STRING: functional protein association networks (string-db.org)) search was performed on MS hits to investigate protein-protein interaction. Using the 'Multiple Proteins' search bar, the hits associated with either SRF or AR were inputted into the search list (with additional input of AR and SRF also) and searched against the '*Homo sapiens*' database.

3-(4,5)-dimethylthiazol-2-yl-2,5-diphenlytetrazolium bromide (MTT) cell viability assay

Three thousand cells per well were cultured in 96 well plates. Cells were treated with increasing concentrations of either JG-98, Ver-155008, Ganetispib, Ipatasertib or Alpelisib or DMSO control. Cells were treated for 5 days followed by MTT analysis as previously described [15].

Statistical analysis

IC_{50} values were calculated using a non-linear regression dose response curve on Graphpad Prism version 7. Unpaired two-tailed Student's t-tests were performed to compare treated conditions with the vehicle control. P values below 0.05 were considered statistically significant. All tests are indicated in the table legends.

Results

Interactome analysis identifies AR and SRF common interactors

As already mentioned, studies have shown that there is an indirect relationship between the SRF and AR pathways. As both SRF and AR are master transcriptional regulators, their transcriptional prowess relies on the presence of various co-factors. Hence, we used Co-IP and MS to identify the common co-factors that bind to both SRF and AR. The experimental design for

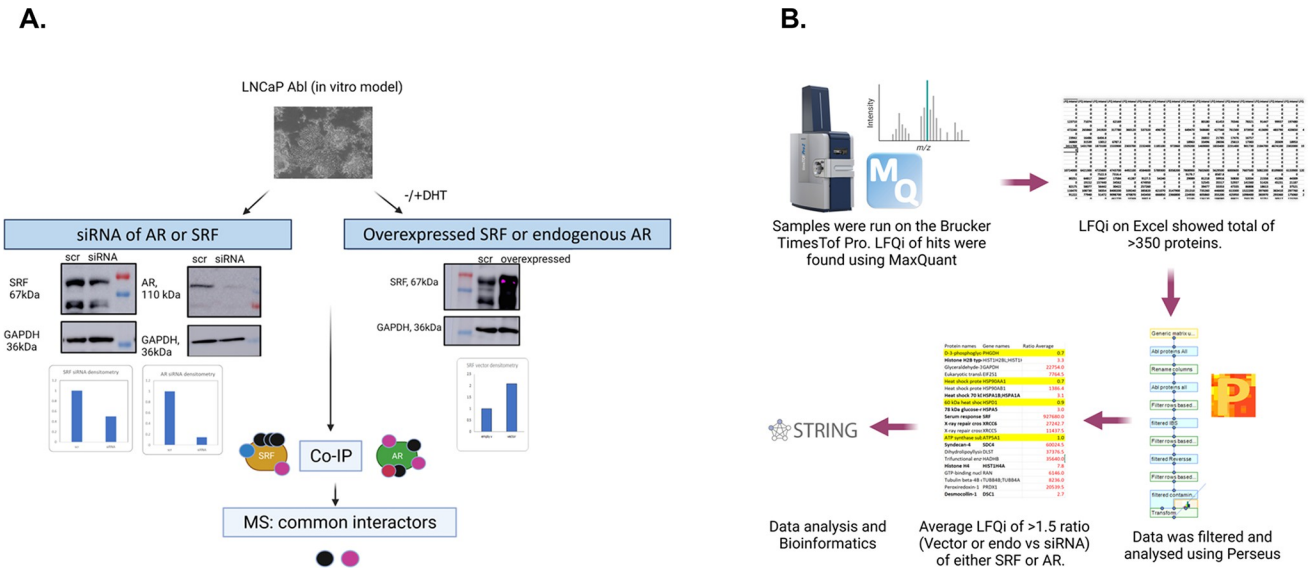

Fig 1. Discovery approach to identify the common interactors in the SRF and AR pathways. A. Schematic diagram of the experimental design. LNCaP Abl cells were transfected with either scramble siRNA, AR siRNA, SRF siRNA or with a plasmid overexpressing SRF, with or without DHT stimulation. LC-MS was performed following Co-IP pulldowns with antibodies specific for AR or SRF. B. Schematic diagram of data analysis following MS.

https://doi.org/10.1371/journal.pone.0309491.g001

this discovery approach is outlined in Fig 1. LNCaP Abl cells were transfected with scrambled siRNA, AR siRNA or SRF siRNA, and SRF vector in the presence or absence of 10nM DHT (for 24 hours) before pulldown. DHT stimulation was introduced to enrich for co-factors involved in transcriptional regulation of AR. The siRNA samples were used as a negative control to eliminate any non-specific interactors during data analysis. Overexpression of SRF enhanced binding of interactors that would be otherwise missed, while AR is already overexpressed in LNCaP Abl cells [12]. SRF and AR downregulation and SRF overexpression were confirmed by WB (Fig 2). 168 proteins for the AR pull down and 157 for the SRF pull down

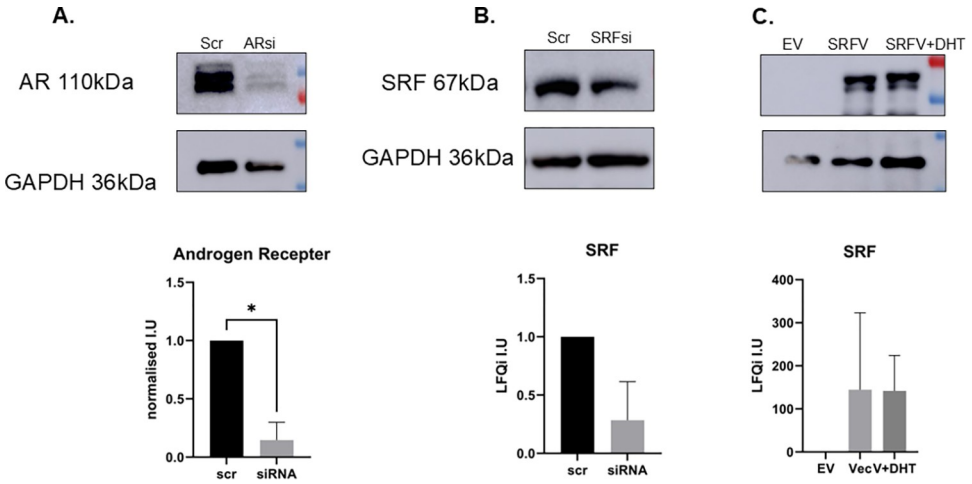

Fig 2. WB validation of downregulation of AR and SRF and upregulation of SRF following siRNA/plasmid transfections. Top panels show WB representative images of three independent experiments. Bottom panels show densitometry analysis of WB images. A. AR down-regulation; B. SRF down-regulation; C. SRF up-regulation. Bars represent average of three independent experiments ± standard deviation. Abbrev: Scr = scrambled, EV = empty vector, SRFV = SRF overexpressing vector, SRFV+DHT = SRF overexpressing vector + DHT. Two-tailed t-test was carried out followed by Welch's correction. * = $p<0.05$.

https://doi.org/10.1371/journal.pone.0309491.g002

were identified before and after DHT combined (S1 and S2 Tables). The data obtained from MaxQuant was analysed on Perseus software to remove contaminants and reverse proteins, which are generally defined as CrapOME, nonspecific for proteomic analysis [16] and could be false positives or nonbiological protein sequences respectively. Proteins that did not appear in at least two of the three biological replicates were discarded. LFQi ratios of either AR endogenous (with and without DHT stimulation) *vs*. AR siRNA, or SRF overexpression *vs*. SRF siRNA (with and without DHT stimulation) were calculated for each independent experiment.

To identify the proteins with increased expression in the overexpressed (SRF) or endogenous (AR) samples compared to siRNA, LFQi ratios were used to obtain a cut-off of $\geq$1.5 of overexpression/siRNA or endogenous/siRNA, in line with previous proteomic studies on the AR interactome [17]. Twenty-one proteins interacting with SRF were identified before DHT and 14 post-DHT stimulation (Fig 3, panel A). From the AR Co-IP, 10 proteins were identified before DHT and 6 after DHT stimulation (Fig 3, panel B). AR and SRF datasets were then analysed for common interactors. A total of 7 proteins were identified in all datasets (Table 1). The 7 common interactors include Heat-shock 70kDa protein (HSP70), Heat-shock protein 90α (HSP90α) and Heat-shock protein 90β (HSP90β), 78 kDa glucose-regulated protein (HSPA5) and Heat-shock cognate 71 kDa (HSPA8), Glyceraldehyde 3-phosphatase (GAPDH) and the antioxidant enzyme peroxiredoxin-1 (PRDX1). Interestingly, 5 of these proteins interacted with both AR and SRF without DHT stimulation (HSP70, HSP0AA1, HSP90AB1, HSPA5, PRDX1), there were no common proteins associated with AR and SRF after DHT

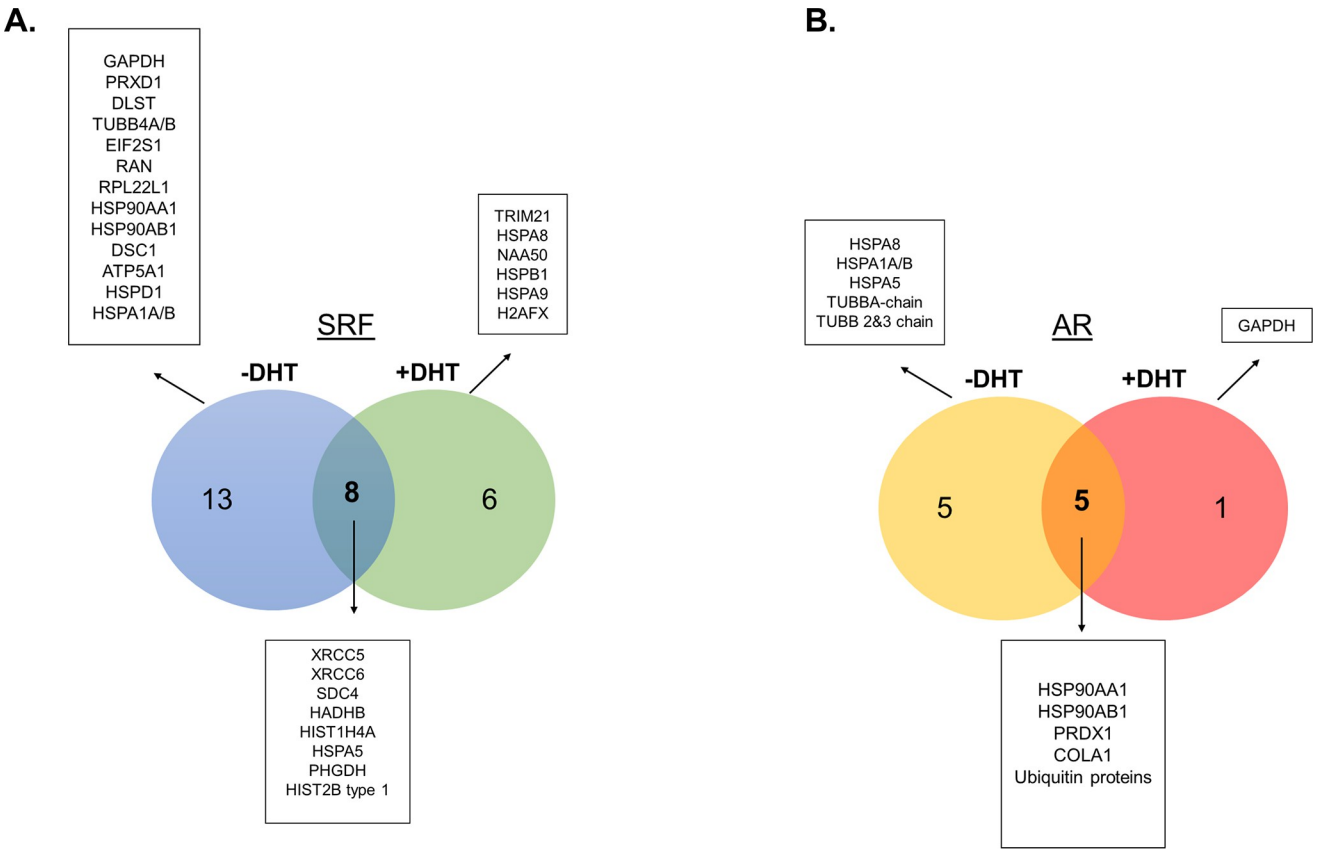

Fig 3. Summary of the identified proteins in different experimental groups. A) Proteins from the SRF dataset before and after DHT. B) Proteins from the AR dataset before and after DHT.

https://doi.org/10.1371/journal.pone.0309491.g003

Table 1. List of AR/SRF common interactors, and their functions taken from Uniprot (Uniprot KB/Swiss-Prot).

AR/SRF Common interactors		
Protein names	**Gene names**	**Function (Uniprot Swiss-Prot)**
Heat shock 70 kDa protein	HSPA1B; HSPA1A	Molecular Chaperone Protein involved in protein degradation and re-folding
Heat shock protein HSP 90-alpha*	HSP90AA1	Chaperone protein that regulates proteins involved in cell cycle control and signal transduction
Heat shock protein HSP 90-beta	HSP90AB1	HSP90 subunit
78 kDa glucose-regulated protein	HSPA5	Endoplasmic reticulum chaperone protein
Heat shock cognate 71 kDa protein*	HSPA8	Molecular chaperone protein
Glyceraldehyde-3-phosphate dehydrogenase	GAPDH	Key enzyme in glycolysis
Peroxiredoxin-1	PRDX1	Protects cells from oxidative stress

https://doi.org/10.1371/journal.pone.0309491.t001

stimulation, and 2 proteins were in common to SRF and AR at different DHT stimulation status (GAPDH interacted with SRF -DHT and AR +DHT and HSPA8 interacted with SRF +DHT and AR -DHT).

Pathway analysis of the AR/SRF common interactors

The common interactors of AR/SRF were analysed using STRING to identify other pathways in the interactome that may be vulnerable to inhibitors (Fig 4, panel A). This analysis identified proline, glutamate and leucine rich protein 1 (PELP-1), a steroid nuclear receptor adaptor protein that has known interactions with both AR and SRF [18]. Additionally, CTNNB1 (or β-catenin), a major component of the WNT signalling pathway, has been shown to interact with AR and weakly associated with SRF [18, 19]. Using the expansion method on the STRING database with the common AR/SRF interactors as the input, enriched pathways were investigated, using the KEGG database. PI3k-Akt and MAPK signalling pathways resulted significantly enriched in this analysis (False Discovery Rate, FDR<0.05) (Fig 4, panel B).

Functional validation of the proteins identified in the AR/SRF interactome

The MS data coupled with bioinformatic analysis identified several interesting targets, summarised in Table 2. HSP70, HSP90 and AKT signalling were prioritised for further functional validation. The drugs tested included the HSP70 inhibitors, Ver-155008 and JG-98, HSP90 inhibitor Ganetespib, PI3k inhibitor Alpelisib and AKT inhibitor Ipatasertib.

The rationale for starting our functional investigation from these three targets is as follows. Inhibition of HSP70 in pre-clinical models of CRPC has shown promise in its capability as therapeutic target and in overcoming resistance to AR antagonists [20]. HSP90 is a known AR coregulator [21] that is regulated by HSP27, which contains Serum Responsive Elements in its promoter region, and therefore is potentially under the transcriptional control of SRF [22], making it an ideal target in the context of our study. Moreover, HSP90 inhibition in combination with ADT is currently being investigated in clinical trials (Trials: NCT0168526 and NCT01270880). One of these trials include the HSP90 inhibitor, Ganetespib, which was tested in patients with CRPC [23] but was not deemed efficient as a single drug, therefore our study may offer novel avenues for combination treatments. As the PI3k/AKT signalling is upstream of both AR and SRF and emerged as an enriched pathway in the STRING analysis, we also tested Ipatasertib and Alpelisib. Ipatasertib is an AKT inhibitor that is in phase III clinical trials in combination with abiraterone acetate for mCRPC (NCT03072238) and for CRPC patients

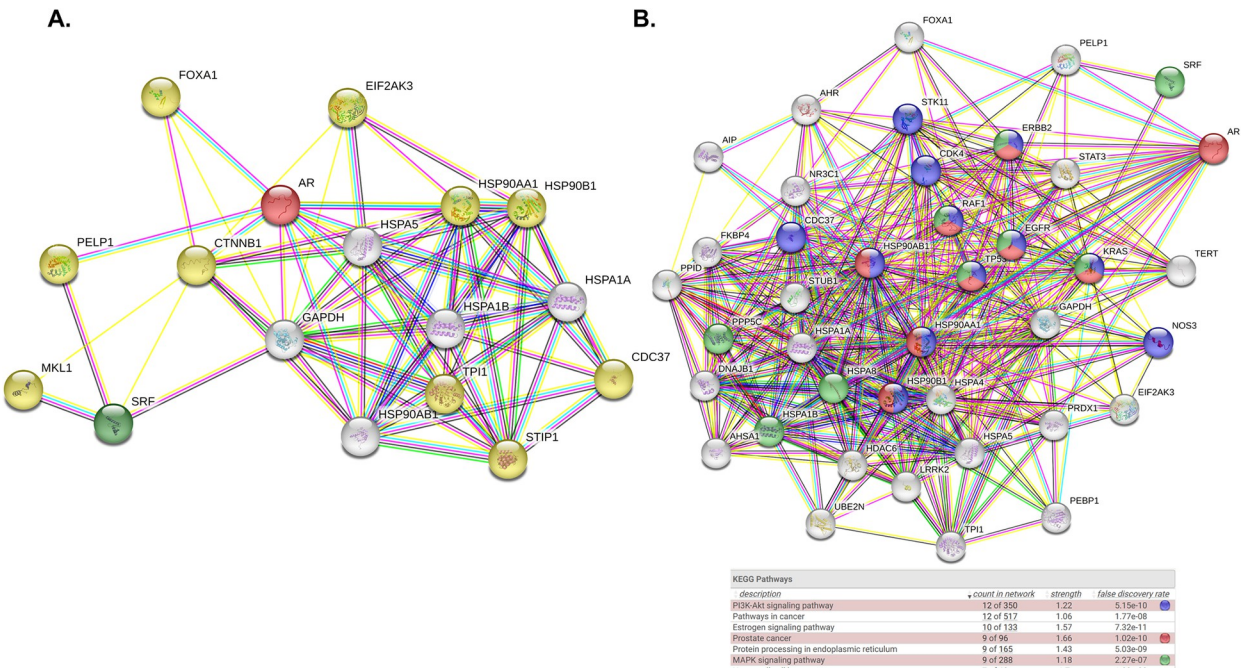

Fig 4. Pathway and network analysis of the proteins identified in the AR/SRF interactome. STRING analysis of the common interactors between SRF and AR revealed other proteins involved in the AR/SRF interactome. A. Common interactors and their known interactions with AR and SRF. Common interactor nodes are shown in white. AR and SRF nodes are shown in red and green respectively. Yellow nodes represent other proteins following network expansion. B) Following network expansion, a list of highly significant KEGG pathways were highlighted. Blue nodes represent proteins involved in the PI3k-Akt pathways, red nodes proteins involved in prostate cancer signalling, and green nodes MAPK signalling pathway. The highlighted pathways all have a false discovery ratio below 0.05. The thickness of the lines between proteins indicates the strength of data support.

https://doi.org/10.1371/journal.pone.0309491.g004

that developed resistance to docetaxel (NCT01485861) [24]. Among the numerous PI3k inhibitors currently available, we selected Alpelisib, which targets the *PI3KCA* mutation, associated with poor survival in patients with PCa [25].

Table 2. List of molecular targets identified through MS and STRING analysis.

Target	Gene ID	Function	Inhibitor(s)	Clinical Trial ID
Heat Shock protein 90	HSP90AA1 HSP90AB1	AR co-regulator and chaperone protein	Onalespib Ganetespib Luminespib	NCT01685268 (met PCa with ADT) NCT01270880 (met PCa)
HSP70 family of proteins	HSPA1/B; HSPA5; HSPA9	Chaperone proteins	VER-155008	Pre-clinical models
			JG-98 series of HSP70 inhibitors	
Ku70/80	XRCC5 and XRCC6	AR co-regulator, DNA repair protein	Vitas-M STL127705	n/a
Tubulin beta chain IV and chain II	TUBB4 and TUBB2	Constituent of microtubules	Tubulin Inhibitors (eg docetaxel, cabazitaxel, vinblastine,	Many clinical trials with docetaxel and cabazitaxel for met PCa.
				ABT-751
Peroxiredoxin-1	PRDX1	Antioxidant enzyme	PRDX1 Inhibitor H7	n/a
PELP-1	PELP1	AR co-regulator, adaptor protein	Peptidomimetics*	Preclinical models
PI3k complex	PIK3CA	Activates multiple intracellular signaling pathways	Alpesilib	n/a
Akt	AKT1	Tyrosine kinase pathway	Ipatasertib	NCT03072238 (met PCa with ADT) NCT01485861 (met PCa)
			ONC-201 (ERK/Akt inhibitor)	
				Phase 3 GBM

https://doi.org/10.1371/journal.pone.0309491.t002

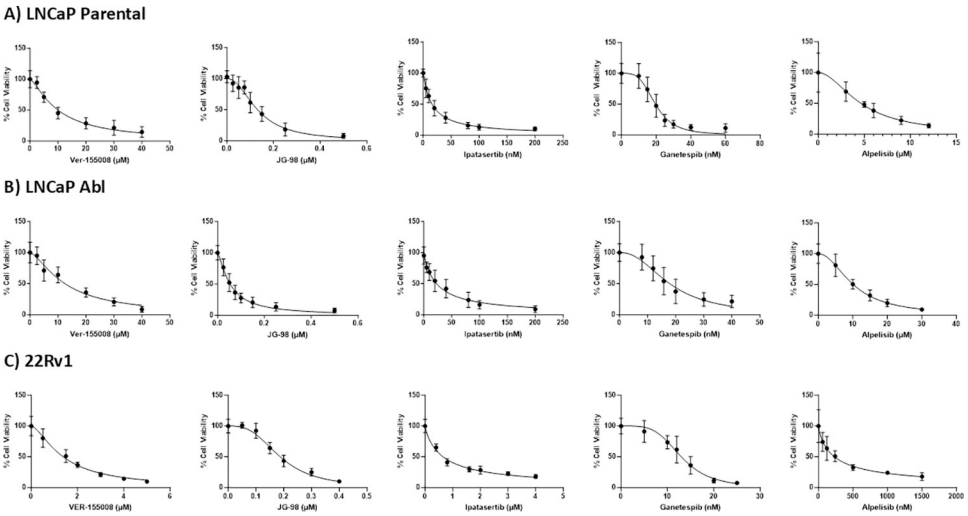

Fig 5. Cell viability graphs of inhibitors against HSP70, HSP90, PI3k and AKT. Dose dependent curves of inhibitors Ver-155008, JG-98, Ipatasertib, Ganetespib and Alpelisib. A) LNCaP Parental. Concentrations used are as follows: Ver-155008 (μM): 0, 2.5, 5, 10, 20, 30, 40. JG-98 (μM): 0, 0.025, 0.050, 0.075, 0.1, 0.15, 0.25, 0.5. Ipatasertib (nM): 0, 5, 10, 20, 20, 40, 80, 100, 200. Ganetespib (nM): 0, 10, 20, 15, 20, 30, 40, 60. Alpelisib (μM): 0, 3, 6, 9, 12 B) LNCaP Abl. Concentrations used are as follows: Ver-155008 (μM): 0, 2.5, 5, 10, 20, 30, 40. JG-98 (μM): 0, 0.025, 0.05, 0.075, 0.1, 0.15, 0.25, 0.5. Ipatasertib (nM): 0, 5, 10, 20, 40, 80, 100, 200. Ganetespib (nM): 0, 8, 12, 15.8, 20, 30, 40. Alpelisib (μM): 0, 1, 5, 15, 20. C) 22Rv1. Concentrations used are as follows: Ver-155008 (μM): 0, 0.5, 1.5, 2, 3, 4, 5. JG-98 (μM): 0, 0.05, 0.1, 0.15, 0.2, 0.3, 0.4. Ipatasertib (μM): 0, 0.4, 0.8, 1.6, 2, 3, 4. Ganestespib (nM): 0, 5, 10, 12, 15, 20, 25. Alpelisib (nM): 0, 60, 120, 240, 500, 1000, 1500, 3000. For each inhibitor, graphs represent the average of at least three biological replicates in triplicate. Error bars represent standard deviation.

https://doi.org/10.1371/journal.pone.0309491.g005

Following 5 days of treatment, viability was assessed using MTT assays. In the Parental cells, IC_{50} concentrations were as follows: 10.3 ±1.7 μM for Ver-155008, 0.13 ±0.13 μM for JG-98, 17.2 ±7.9nM for Ipatasertib, 19.9 ±2 nM for Ganetespib and 4.7 ±1μM for Alpelisib (Fig 5, panel A, Table 3). Despite both drugs have HSP70 as a target, the IC_{50} concentration of JG-98 was lower than that of Ver-155008, possibly due to different mechanisms of action of these drugs. In the LNCaP Abl cells, the IC_{50} concentrations of Ver-155008 was 12.5 ±4.1μM, JG-98 was 70 ±30 nM, Ipatasertib was 25.6 ±13.6 nM, Ganetespib was 18.7 ±6.7nM and Alpelisib was 10.18 ±1μM (Fig 5, panel B, Table 4). In the 22rv1 cells, the IC_{50} concentrations of Ver-155008 was 1.5 ±0.2μM, JG-98 was 191.7 ±16.8nM, Ipatasertib was 639.1 ±11.3nM, Ganetespib was 13 ±1.9nM and Alpelisib was 234.7 ±50.8nM (Fig 5, panel C, Table 5). Interestingly, the IC_{50} values of all the drugs tested (excluding Ver-155008) were significantly lower than that of enzalutamide previously reported in LNCaP parental cells (8.8 ±3.4 μM) [15]. In the Abl cell line, which models CRPC, the IC_{50} values of all the drugs texted were also significantly lower than

Table 3. IC_{50} values of inhibitors compared against enzalutamide in LNCaP parental cells. IC_{50} values represent averages of at least three independent experiments in triplicate. One-Way-ANOVA was carried out on each drug, followed by Tukey's test to compare the mean IC_{50} value against the mean IC_{50} value of enzalutamide.

	IC_{50} values (μM/nM)	Standard Deviation	P value
Enzalutamide	8.8μM	3.4μM	-
Ver-155008	10.3μM	1.7μM	ns
JG-98	0.13μM	0.13μM	<0.0001
Ipatasertib	17.2nM	7.9nM	<0.0001
Ganetespib	19.9nM	2nM	<0.0001
Alpelisib	4.7μM	1μM	<0.001

https://doi.org/10.1371/journal.pone.0309491.t003

Table 4. IC_{50} values of inhibitors compared against enzalutamide in the LNCaP Abl cells. IC_{50} values represent averages of at least three independent experiments in triplicate. One-Way-ANOVA was carried out on each drug, followed by Tukey's test to compare the mean IC_{50} value against the mean IC_{50} value of enzalutamide.

	IC_{50} values (μM/nM)	Standard Deviation	P value
Enzalutamide	26.3μM	6.9μM	-
Ver-155008	12.5μM	4.1μM	<0.0001
JG-98	70nM	30nM	<0.0001
Ipatasertib	25.6nM	13.6nM	<0.0001
Ganetespib	18.7nM	6.7nM	<0.0001
Alpelisib	19.18μM	1μM	<0.0001

https://doi.org/10.1371/journal.pone.0309491.t004

that of enzalutamide (26.3 ±6.9 μM). An IC_{50} was not found for the 22rv1 because these cells are resistant to enzalutamide, probably due the presence of the ARv7 variant. For these cells we compared all the drugs to EPI-7170, which targets both ARv7 and AR full length. All the IC_{50} were significantly lower than EPI-7170.

Discussion

In this study 21 proteins were detected in the SRF Co-IP before DHT stimulation and 14 proteins after DHT stimulation. Among them there were XRCC5 and XRCC6, also known as Ku80 and Ku70, heterodimeric DNA repair proteins involved in non-homologous end joining of dsDNA breaks in the cell [26]. Ku70/80 are known AR co-activators and aid in its nuclear translocation in LNCaP cells, particularly in the presence of DHT. Their interaction with SRF, a master regulator of actin filaments [22], happens through polymerised F-actin, which is vital for Ku70 localisation and Ku80 stabilisation during dsDNA breaks [26]. Another AR known co-activator that co-precipitated with SRF is RAN, also known as ARA24. RAN is a nucleocytoplasmic protein that directly binds to the NH2-COOH transcription activating domain of the AR protein [27]. Significantly increased RAN expression in PCa samples compared to normal adjacent samples was demonstrated. Additionally, RAN colocalization with AR was predominantly observed in the nucleus and was enhanced in the presence of DHT, suggesting that RAN is particularly important in AR nuclear compartmentalisation and transcriptional activation [27].

Pathway analysis of the MS hits of the AR/SRF interactome, lead to other potential common interactors, including the AR coactivator and adaptor protein PELP-1 and β-catenin. PELP-1 interaction with SRF was previously shown in NIH3T3 cells, where PELP-1 acts as a corepressor of SRF transcriptional activity [28]. PELP-1 is also a coregulator of nuclear steroid transcription factors and is involved in cell cycle progression, playing an oncogenic role in breast and prostate cancer [29]. Supporting our STRING analysis, a study of the AR interactome

Table 5. IC_{50} values of inhibitors compared against EPI-7170 in the 22rv1 cells. IC_{50} values represent averages of at least three independent experiments in triplicate. One-Way-ANOVA was carried out on each drug, followed by Tukey's test to compare the mean IC_{50} value against the mean IC_{50} value of EPI-7170.

	IC_{50} values (μM/nM)	Standard Deviation	P value
EPI-7170	9.209 μM	2.62 μM	-
Ver-155008	1.523 μM	0.2 μM	< 0.01
JG-98	191.7 nM	16.8 nM	< 0.001
Ipatasertib	639.1 nM	11.35 nM	< 0.01
Ganetespib	13.00 nM	1.874 nM	< 0.01
Alpelisib	234.7 nM	50.84 nM	< 0.01

https://doi.org/10.1371/journal.pone.0309491.t005

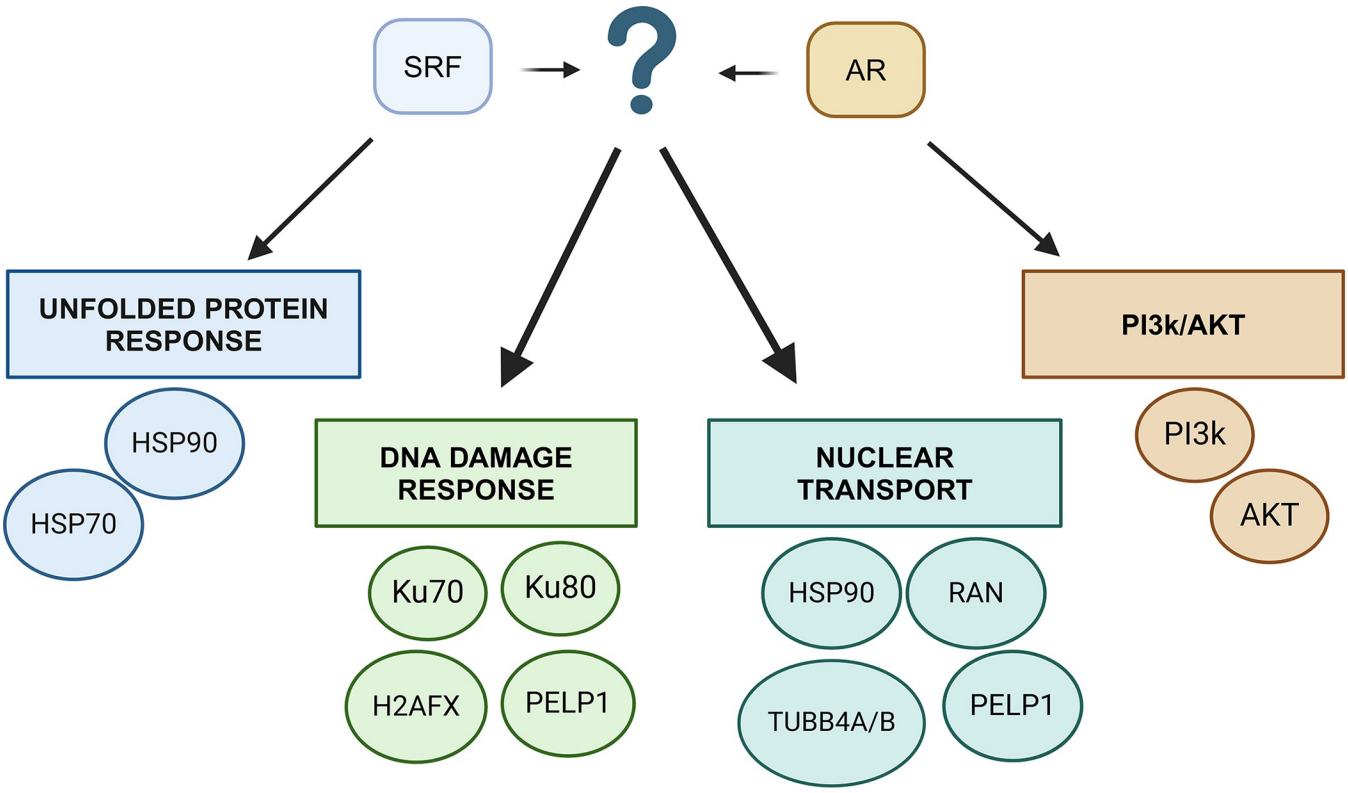

Fig 6. Proposed common pathways of the SRF/AR interactome and the key proteins identified by APMS and bioinformatics.

https://doi.org/10.1371/journal.pone.0309491.g006

showed that PELP-1 and β-catenin were significantly upregulated in PCa tumour compared to normal tissue [30]. Despite its large molecular weight, peptidomimetics against PELP-1 in primary PCa explants and PCa xenografts have shown promise in disrupting AR translocation to the nucleus, resulting in decreased AR-mediated transcription [28].

The PI3k/AKT pathway emerged as the most enriched pathway following expansion of STRING analysis when all the 7 common interactors were inputted. This pathway is aberrant in many different cancers and leads to enhanced cell proliferation and resistance to apoptotic cell death [24]. Inhibitors of AKT such as Capavisertib and Ipatasertib have shown promise as combination treatment with ADT in patients with CRPC and PTEN loss [24]. Importantly, a crosstalk has been established between AR and the PI3k/AKT pathway in PCa, with the PI3k/AKT pathway activated in 42% of localised PCa cases and 100% in advanced forms of disease [24]. Furthermore, inhibition of AR leads to overexpression of the PI3k/AKT pathway leading to aggressive growth, metastases and resistance to treatments. A downstream target of this pathway, mTOR, was shown to regulate the expression of HMMR in PCa cells via SRF, suggesting a possible link between the PI3k/AKT/AR/SRF pathways in PCa. Overall, we propose four possible common pathways in the SRF/AR interactome as detailed in Fig 6.

Out of our list of possible targets in the AR/SRF pathway, HSP90, HSP70, AKT and PI3K were functionally validated using Ganetespib, VER-155008/JG-98, Ipatasertib and Alpelisib respectively. Our results verified that inhibition of these proteins reduced cell viability in both LNCaP parental and Abl cells. Their IC50 values were significantly lower than that of enzalutamide, suggesting promise for further investigation. Specifically, combinations of inhibitors of key proteins in the AR/SRF signalling pathways with current therapies targeting AR and SRF inhibitors, may result in synergy in decreasing cell viability and proliferation, limiting PCa

progression. When designing combination treatments, it is vital to fully explore the mechanisms of action of each drug, and whether synergy occurred *in vitro*, and in pre-clinical models. A few factors ought to be considered, such as the dose, timing of the drug and the potential pathways affected. Although *in vitro* work demonstrates synergy when combining inhibitors, these findings may not translate well in patients. For example, a phase I clinical trial reported that combining PARP inhibitor olaparib with cisplatin in patients with solid tumours led to severe myelosuppression (NCT00782574) [31] and was deemed intolerable. This effect was also observed in another phase I trial combining olaparib and cisplatin with gemcitabine, even at low doses [32]. However, combination of PARP with cisplatin in *in vitro* models of ovarian cancer demonstrated synthetic lethality [33]. Instead of focusing on combining current treatments that have off-target effects, inhibition of specific pathways that influence each other, such as DNA repair and PI3k/AKT pathway, may help reduce toxicity and lead to tumour cell death. The ComPAKT trial explored the inhibition of PARP and AKT in patients with solid tumours [34] and showed that combination of inhibitors that target specific pathways have better pharmacokinetics and are well tolerated at higher doses. Thereby, understanding how two pathways influence one another, whether directly or indirectly, is essential in the planning of combination treatments. Further research is needed to explore the molecular mechanisms of how our findings tie in with the AR/SRF crosstalk in CRPC.

Supporting information

S1 Table. List of peptides precipitated with AR. Numbers indicate LFQi values. Abbreviations: AR KD, AR knocked down; AR ENDO, endogenous AR.
(DOCX)

S2 Table. List of peptides precipitated with SRF. Numbers indicate LFQi values. Abbreviations: SRF KD, SRF knockdown; SRF Vec, SRF upregulation vector.
(DOCX)

S1 Raw images. Uncropped WB images.
(PDF)

Acknowledgments

The authors would like to thank the Conway Institute mass spectrometry core facility, especially Dr Caitriona Scaife, Dr Eugene Dillon and Dr Kieran Wynne.

Author Contributions

Conceptualization: Simone Marcone, Maria Prencipe.

Data curation: Haleema Azam, Maria Prencipe.

Formal analysis: Haleema Azam.

Funding acquisition: Maria Prencipe.

Investigation: Haleema Azam, Colin Veale, Kim Zitzmann.

Methodology: Haleema Azam.

Project administration: Maria Prencipe.

Supervision: Simone Marcone, William M. Gallagher, Maria Prencipe.

Writing – original draft: Haleema Azam.

Writing – review & editing: Colin Veale, Kim Zitzmann, Simone Marcone, William M. Gallagher, Maria Prencipe.

References

1. Wang Y, Chen J, Wu Z, Ding W, Gao S, Gao Y et al. Mechanisms of enzalutamide resistance in castration-resistant prostate cancer and therapeutic strategies to overcome it. *Br J Pharmacol*. 2021; 178 (2):239–261. https://doi.org/10.1111/bph.15300 PMID: 33150960
2. Tien AH, Sadar MD. Keys to unlock androgen receptor translocation. *J Biol Chem*. 2019; 294 (22):8711–8712. https://doi.org/10.1074/jbc.H119.009180 PMID: 31152093
3. Verone AR, Duncan K, Godoy A, Yadav N, Bakin A, Koochekpour S et al. Androgen-responsive serum response factor target genes regulate prostate cancer cell migration. *Carcinogenesis*. 2013; 34 (8):1737–1746. https://doi.org/10.1093/carcin/bgt126 PMID: 23576568
4. Prencipe MO'Neill A, O'Hurley G, Nguyen LK, Fabre ABjartell A, et al. Relationship between serum response factor and androgen receptor in prostate cancer. *The Prostate*. 2015; 75(15):1704–1717. https://doi.org/10.1002/pros.23051 PMID: 26250344
5. Venkadakrishnan VB, DePriest AD, Kumari S, Senapati D, Ben-Salem S, Su Y, et al. Protein Kinase N1 control of androgen-responsive serum response factor action provides rationale for novel prostate cancer treatment strategy. *Oncogene*. 2019; 38(23):4496–4511. https://doi.org/10.1038/s41388-019-0732-7 PMID: 30742064
6. Heemers HV, Schmidt LJ, Sun Z, Regan KM, Anderson SK, Duncan K, et al. Identification of a Clinically Relevant Androgen-Dependent Gene Signature in Prostate Cancer. *Cancer Res*. 2011; 71(5):1978–1988. https://doi.org/10.1158/0008-5472.CAN-10-2512 PMID: 21324924
7. Kollara A, Brown TJ. Modulation of aryl hydrocarbon receptor activity by four and a half LIM domain 2. *Int J Biochem Cell Biol*. 2009; 41(5):1182–1188. https://doi.org/10.1016/j.biocel.2008.10.019 PMID: 19015043
8. Cao CY, Mok SWF, Cheng VWS, Tsui SKW. The FHL2 regulation in the transcriptional circuitry of human cancers. *Gene*. 2015; 572(1):1–7. https://doi.org/10.1016/j.gene.2015.07.043 PMID: 26211626
9. Miano JM. Serum response factor: toggling between disparate programs of gene expression. *J Mol Cell Cardiol*. 2003; 35(6):577–593. https://doi.org/10.1016/s0022-2828(03)00110-x PMID: 12788374
10. Watson RW, Azam H, Aura C, Russell N, McCormack J, Corey E, et al. Inhibition of Serum Response Factor Improves Response to Enzalutamide in Prostate Cancer. *Cancers*. 2020; 12(12):3540. https://doi.org/10.3390/cancers12123540 PMID: 33260953
11. Salem O, Jia S, Qian BZ, Hansen CG. AR activates YAP/TAZ differentially in prostate cancer. Life Sci Alliance. 2023 Jun 29; 6(9):e202201620. https://doi.org/10.26508/lsa.202201620 PMID: 37385752
12. Culig Z, Hoffmann J, Erdel M, Eder IE, Hobisch A, Hittmair A, et al. Switch from antagonist to agonist of the androgen receptor bicalutamide is associated with prostate tumour progression in a new model system. *Br J Cancer*. 1999; 81(2):242–251. https://doi.org/10.1038/sj.bjc.6690684 PMID: 10496349
13. Cox J, Mann M. MaxQuant enables high peptide identification rates, individualized p.p.b.-range mass accuracies and proteome-wide protein quantification. *Nat Biotechnol*. 2008; 26(12):1367–1372. https://doi.org/10.1038/nbt.1511 PMID: 19029910
14. Tyanova S, Temu T, Sinitcyn P, Carlson A, Hein MY, Geiger T, et al. The Perseus computational platform for comprehensive analysis of (prote)omics data. *Nat Methods*. 2016; 13(9):731–740. https://doi.org/10.1038/nmeth.3901 PMID: 27348712
15. Azam H, Maher S, Clarke S, Gallagher WM, Prencipe M. SRF inhibitors reduce prostate cancer cell proliferation through cell cycle arrest in an isogenic model of castrate-resistant prostate cancer. *Cell Cycle Georget Tex*. 2023; 22(14–16):1759–1776. https://doi.org/10.1080/15384101.2023.2229713 PMID: 37377210
16. Mellacheruvu D, Wright Z, Couzens AL, Lambert JP, St-Denis NA, Li T, et al. The CRAPome: a contaminant repository for affinity purification-mass spectrometry data. *Nat Methods*. 2013; 10(8):730–736. https://doi.org/10.1038/nmeth.2557 PMID: 23921808
17. Xue C, Corey E, Gujral TS. Proteomic and Transcriptomic Profiling Reveals Mitochondrial Oxidative Phosphorylation as Therapeutic Vulnerability in Androgen Receptor Pathway Active Prostate Tumors. *Cancers*. 2022; 14(7):1739. https://doi.org/10.3390/cancers14071739 PMID: 35406510
18. Yang L, Ravindranathan P, Ramanan M, Kapur P, Hammes SR, Hsieh JT, et al. Central role for PELP1 in nonandrogenic activation of the androgen receptor in prostate cancer. *Mol Endocrinol Baltim Md*. 2012; 26(4):550–561. https://doi.org/10.1210/me.2011-1101 PMID: 22403175
19. Murillo-Garzón V, Kypta R. WNT signalling in prostate cancer. *Nat Rev Urol*. 2017; 14(11):683–696. https://doi.org/10.1038/nrurol.2017.144 PMID: 28895566

20. Xu P, Yang JC, Ning S, Chen B, Nip C, Wei Q, et al. Allosteric inhibition of HSP70 in collaboration with STUB1 augments enzalutamide efficacy in antiandrogen resistant prostate tumor and patient-derived models. *Pharmacol Res*. 2023; 189:106692. https://doi.org/10.1016/j.phrs.2023.106692 PMID: 36773708

21. Veldscholte J, Berrevoets CA, Ris-Stalpers C, Kuiper GGJM, Jenster G, Trapman J, et al. The androgen receptor in LNCaP cells contains a mutation in the ligand binding domain which affects steroid binding characteristics and response to antiandrogens. *J Steroid Biochem Mol Biol*. 1992; 41(3):665–669. https://doi.org/10.1016/0960-0760(92)90401-4 PMID: 1562539

22. Miano JM, Long X, Fujiwara K. Serum response factor: master regulator of the actin cytoskeleton and contractile apparatus. *Am J Physiol Cell Physiol*. 2007; 292(1):C70–81. https://doi.org/10.1152/ajpcell.00386.2006 PMID: 16928770

23. Ben-Salem S, Venkadakrishnan VB, Heemers HV. Novel insights in cell cycle dysregulation during prostate cancer progression. *Endocr Relat Cancer*. 2021; 28(6):R141–R155. https://doi.org/10.1530/ERC-20-0517 PMID: 33830069

24. Tortorella E, Giantulli S, Sciarra A, Silvestri I. AR and PI3K/AKT in Prostate Cancer: A Tale of Two Interconnected Pathways. *Int J Mol Sci*. 2023; 24(3):2046. https://doi.org/10.3390/ijms24032046 PMID: 36768370

25. Pearson HB, Li J, Meniel VS, Fennell CM, Waring P, Montgomery KG, et al. Identification of Pik3ca Mutation as a Genetic Driver of Prostate Cancer That Cooperates with Pten Loss to Accelerate Progression and Castration-Resistant Growth. *Cancer Discov*. 2018; 8(6):764–779. https://doi.org/10.1158/2159-8290.CD-17-0867 PMID: 29581176

26. Al-Ubaidi FLT, Schultz N, Loseva O, Egevad L, Granfors T, Helleday T. Castration therapy results in decreased Ku70 levels in prostate cancer. *Clin Cancer Res Off J Am Assoc Cancer Res*. 2013; 19(6):1547–1556. https://doi.org/10.1158/1078-0432.CCR-12-2795 PMID: 23349316

27. Harada N, Ohmori Y, Yamaji R, Higashimura Y, Okamoto K, Isohashi F, et al. ARA24/Ran enhances the androgen-dependent NH2- and COOH-terminal interaction of the androgen receptor. *Biochem Biophys Res Commun*. 2008; 373(3):373–377. https://doi.org/10.1016/j.bbrc.2008.06.024 PMID: 18565325

28. Choi YB, Ko JK, Shin J. The transcriptional corepressor, PELP1, recruits HDAC2 and masks histones using two separate domains. *J Biol Chem*. 2004; 279(49):50930–50941. https://doi.org/10.1074/jbc.M406831200 PMID: 15456770

29. Gonugunta VK, Miao L, Sareddy GR, Ravindranathan P, Vadlamudi R, Raj GV. The social network of PELP1 and its implications in breast and prostate cancers. *Endocr Relat Cancer*. 2014; 21(4):T79–86. https://doi.org/10.1530/ERC-13-0502 PMID: 24859989

30. Wang Z, Zhang Y, Deng Q, Zhang J, Wang X, Liang H. Integrative Analysis of Androgen Receptor Interactors Aberrations and Associated Prognostic Significance in Prostate Cancer. *Urol J*. 2023; 20:1–6. https://doi.org/10.22037/uj.v20i.7469 PMID: 37667572

31. Balmaña J, Tung NM, Isakoff SJ, Graña B, Ryan PD, Saura C, et al. Phase I trial of olaparib in combination with cisplatin for the treatment of patients with advanced breast, ovarian and other solid tumors. Ann Oncol. 2014 Aug; 25(8):1656–63. https://doi.org/10.1093/annonc/mdu187 PMID: 24827126

32. Arun Rajan Corey A Carter; Ronan J. Kelly; Martin Gutierrez; Shivaani Kummar; Eva Szaboet al. A Phase I Combination Study of Olaparib with Cisplatin and Gemcitabine in Adults with Solid Tumors. Clin Cancer Res (2012) 18 (8): 2344–2351. https://doi.org/10.1158/1078-0432.CCR-11-2425 PMID: 22371451

33. Gao J, Wang Z, Fu J, A J, Ohno Y, Xu C. Combination treatment with cisplatin, paclitaxel and olaparib has synergistic and dose reduction potential in ovarian cancer cells. Exp Ther Med. 2021 Sep; 22(3):935. https://doi.org/10.3892/etm.2021.10367 PMID: 34335884

34. Yap TA, Kristeleit R, Michalarea V, Pettitt SJ, Lim JSJ, Carreira S, et al. Phase I Trial of the PARP Inhibitor Olaparib and AKT Inhibitor Capivasertib in Patients with BRCA1/2- and Non-BRCA1/2-Mutant Cancers. Cancer Discov. 2020 Oct; 10(10):1528–1543. https://doi.org/10.1158/2159-8290.CD-20-0163 PMID: 32532747